Conference Extended Paper – Research Article – JTEN – 2014 – 31

Journal of Thermal Engineering
Yildiz Technical University Press, Istanbul, Turkey
Vol. 1, Special Issue 1, pp. 367-380, February, 2015.

http://eds.yildiz.edu.tr/journal-of-thermal-engineering/Articles
Manuscript Received September 26, 2014; Accepted January 03, 2015

This paper was recommended for publication in revised form by Regional Editor Dongsheng Wen

A COMPARATIVE STUDY OF DIFFERENT REACTION MODELS FOR TURBULENT METHANE/HYDROGEN/AIR COMBUSTION

***S.P.R. Muppala**
Faculty of Science, Engineering & Computing
Kingston University
Roehampton Vale, London, UK

B. Manickam
Institut für Technische Verbrennung,
Leibniz Universität Hannover,
Welfengarten 1a, 30167 Hannover, Germany

F. Dinkelacker
Institut für Technische Verbrennung,
Leibniz Universität Hannover,
Welfengarten 1a, 30167 Hannover, Germany

Keywords: reaction rate modelling; turbulent premixed combustion; hydrogen enriched flames molecular transport effects; multi-component flame modelling
* Corresponding author: *SPR Muppala, Tel: +44(0)2084174977*
E-mail address: s.muppala@kingston.ac.uk

ABSTRACT

Reaction modelling of methane/hydrogen combustion has two important aspects. First, such mixtures may be used in future in combustion devices like gas turbines and gas engines in the frame of the demand for efficient energy storage systems, where the amount of hydrogen in natural gas delivering systems may vary according to varying hydrogen production from renewable energies. Second, this can be an important aspect for safety, as such mixtures may occur in disastrous situations and calculations may allow the prediction of safety issues. Modelling of such mixed fuel combustion processes is non-trivial due to the involved preferential diffusion effects, coming from the different diffusivities of methane and hydrogen. In turbulent flame modelling, this topic is of special interest, as also thermo-diffusive instabilities and local influence of the local burning velocity near leading edges of the flame seem to be of importance even for highly turbulent flames. This numerical work deals therefore with a comparative study of five different turbulent combustion models - Bray-Moss-Libby, Linstedt-Vaos (LV), a modified version LV, Turbulent Flamespeed Closure, and Algebraic Flame Surface Wrinkling model - to the situation of turbulent methane/hydrogen/air flames. Validation is done with extensive experimental data obtained by a low swirl burner in the group by Cheng. Besides a basic case with pure methane/air, special emphasis is laid on flames with 40 to 100 % hydrogen content by volume. It is shown that for such methane/hydrogen fuel mixtures common reaction rate models are not sufficient where the fuel effects are included only via a laminar flame speed. Instead, a recently proposed reaction model with the incorporation of an effective Lewis number of the fuel mixture is found to work rather well. This is of both, practical as well as theoretical importance, as for the latter it confirms controversially discussed assumptions of the influence of preferential diffusion.

1. INTRODUCTION

Reaction modelling of turbulent methane/hydrogen combustion has two important aspects. First, such flex-fuel mixtures may be used broadly in future in combustion devices like gas turbines and gas engines. This holds especially with respect to the search for new large scale energy storage systems with respect to strongly varying energy production from renewable energies like wind and solar energy. Here, it is proposed that on peak sun or wind situations electrolytically produced hydrogen may be stored within the existing large scale natural gas delivering and storage system. This chemical energy storage option would allow the allocation of the huge energy capacity needed for the broad use of renewable energies. However, this option would require that the common combustion devices where natural gas is used, like gas turbines or gas engines, are able to operate under varying fuel conditions. For the calculation of such devices suitable reaction models are needed.

Second, also safety aspects of such fuel mixtures are of significant importance. This holds for the energy storage scenario being described before, if such fuel mixtures are released uncontrolled. Even without that, hydrogen safety is a general issue for the chemical industry, for nuclear power plant failures or if the vision of hydrogen delivering systems is followed up. Though hydrogen is a potential energy carrier offering CO_2 free emission during the combustion, this cannot be directly used for combustion due to its high diffusivity, reactivity and burning velocity. Instead, blending hydrogen into hydrocarbon could solve such difficulties. With that, safety issues may be important not only for pure hydrogen but also for hydrogen/methane fuel mixtures. Also here, relevant calculation methods are needed.

An additional aspect is flame stability. The addition of hydrogen to natural gas or methane flames can increase the flame stability in very lean combustion modes. These are of interest for instance in stationary gas turbines due to the ultralow emission characteristics of NOx and soot.

In the current study, therefore the extension of premixed turbulent reaction rate models for hydrogen/methane fuels is investigated in the frame of Reynolds averaged Navier-Stokes (RANS) simulation techniques.

It is well known that hydrogen has a higher reactivity compared to other hydrocarbon fuels. Also the high diffusivity of hydrogen allows this fuel to diffuse faster into the reaction zone. Both effects together are included in increased laminar burning velocities for hydrogen/air flames as well as for hydrogen/hydrocarbon/air flames [1].

For turbulent burning velocities, however, the situation is different. Corresponding to the modelling approach for the averaged reaction rate in turbulent situations that the turbulent reaction rate (and with that the turbulent burning velocity) is the product of a laminar reaction rate (laminar burning velocity) and turbulent flame wrinkling factor as will be described below in Eq. 8, it may be assumed that the modelling of turbulent hydrogen or hydrogen/hydrocarbon combustion can be done similar to that of pure hydrocarbon/air flames, where this wrinkling factor has to be modelled suitable. However, the experimental situation shows that this assumption does not hold. Even for constant turbulence conditions, the addition of hydrogen to the fuel leads to effects not being described alone with the modified laminar burning velocity ([2-7]).

Recent detailed numerical simulation studies (DNS), where three-dimensional turbulent wrinkled flames are calculated in time dependent way, have shown the importance of thermo-diffusive instability effects from the comparative study of three single fuels, propane (with a low diffusion coefficient), methane (with medium diffusion coefficient) and hydrogen (with increased diffusion coefficient) [8]. In a similar study Chakraborty et al. [9] have also shown that the normalized local displacement speed S_d/S_L (which is the factor of interest) depends significantly on the diffusion properties of the fuel. For laminar flame instability studies the Lewis number $Le = \alpha / D$ is commonly used for a simplified description, where α is the thermal diffusivity of the fuel/air mixture and D is the fuel diffusivity (for lean fuel/air mixtures). Both of these properties describe molecular transport processes, being certainly important for the diffusive processes inside laminar premixed flames. However, it was much unexpected that for highly turbulent situations these molecular properties still are of strong significance, as commonly turbulent mixing transport rates are in the order of hundred times greater than molecular transport rates, and are expected to be much more dominant for the overall reaction process [9]. In recent years, however, these influences of molecular transport in turbulent flames have been found in several experimental situations [2, 4, 7] and have also been analyzed numerically [8-10][11] and in theory-based models [12, 13].

The current study investigates the influence of averaged reaction models for hydrogen-hydrocarbon combustion in the frame of the RANS approach with computational fluid dynamics simulation. Several turbulent premixed flame models are compared for measured turbulent hydrogen-hydrocarbon

low swirl flames [5]. These flames operate for a broad range of conditions, as the stability limit is wide.

Two approaches to models are followed. In the first group the mean turbulent reaction rate is modelled as a function of the laminar flame speed (which depends on the hydrogen content) and of turbulence parameters. It will be shown, that none of these models is sufficient to calculate the test cases with enhanced hydrogen content.

In the second part of this work, a modified approach is followed therefore, taking into account additional effects from molecular diffusion. Here a rather simple modification of single fuel models with an effective Lewis number approach allows to calculate essential features of the whole set of experimental data.

2. TURBULENCE & REACTION MODELLING

2.1. Turbulence modelling - RNG κ–ε model

In combustion large density variations occur. For that a density weighted averaging procedure (Favre averaging) is suitable for all the flow and combustion quantities, like, e.g., for velocity:

$$\tilde{u} = \frac{\overline{\rho u}}{\overline{\rho}} \tag{1}$$

being indicated by the tilde. Favre averaged continuity and momentum equations involving turbulent stresses are modelled as

$$\frac{\partial \overline{\rho}}{\partial t} + \frac{\partial}{\partial x_i}(\overline{\rho}\tilde{u}_i) = 0 \tag{2}$$

$$\frac{\partial \tilde{u}_i}{\partial t} + \frac{\partial}{\partial x_i}(\tilde{u}_i \tilde{u}_j) = -\frac{1}{\rho}\frac{\partial \overline{p}}{\partial x_j} + \frac{\partial}{\partial x_i}\left[\nu \frac{\partial \tilde{u}_i}{\partial x_i} - \nu_t\left(\frac{\partial \tilde{u}_i}{\partial x_i} + \frac{\partial \tilde{u}_i}{\partial x_i}\right) - \frac{2}{3}k\delta_{ij}\right] \tag{3}$$

where, ν_t is the turbulent eddy viscosity, given as a function of turbulent quantities:

$$\nu_t = C_\mu \frac{k^2}{\varepsilon} \tag{4}$$

where, $C_\mu = 0.0845$, k and ε are the turbulent kinetic energy and dissipation rate of turbulence. Two additional transport equations are solved for prediction of k and ε and the corresponding transport equations for the RNG k-e turbulence model [14]:

$$\left(\frac{\partial k}{\partial t} + \tilde{u}_i \frac{\partial k}{\partial x_i}\right) = \nu_t S^2 + \frac{\partial}{\partial x_i}\left(\sigma_k \nu_t \frac{\partial k}{\partial x_j}\right) - \varepsilon \tag{5}$$

$$\frac{\partial \varepsilon}{\partial t} + \tilde{u}_i \frac{\partial \varepsilon}{\partial x_i} = C_{\varepsilon 1}\frac{\varepsilon}{k}\nu_t S^2 + \frac{\partial}{\partial x_i}\left(\sigma_\varepsilon \nu_t \frac{\partial \varepsilon}{\partial x_i}\right) - C_{\varepsilon 2}\frac{\varepsilon}{k} - R$$

where

$$S = \sqrt{2 S_{ij} S_{ij}}\ ;\ S_{ij} = \frac{1}{2}\left(\frac{\partial u_i}{\partial x_j} + \frac{\partial u_j}{\partial x_i}\right);\ C_{\varepsilon 1}=1.42;\ C_{\varepsilon 2}=1.68;\ \sigma_k = 1.39 \tag{6}$$

2.2. Reaction modelling

A well-known approach to describe turbulent premixed combustion is represented in terms of a scalar variable c. This reaction progress variable c generalizes reacting species and describes the combustion, which is '0' in reactants and '1' in products. The averaged reaction progress variable $\tilde{c}(x)$ describes the probability to find burnt gas at the position x in the flame. The transport equation for the Favre averaged mean progress variable $\widetilde{c}$, with gradient diffusion model for the scalar flux, is expressed as

$$\frac{\partial}{\partial t}(\overline{\rho}\tilde{c}) + \frac{\partial}{\partial x_k}(\overline{\rho}\widetilde{u_k c}) = \frac{\partial}{\partial x_k}\left(\overline{\rho}\left(\frac{\nu_t}{Sc_t} + \nu\right)\frac{\partial \tilde{c}}{\partial x_k}\right) + \overline{\dot{w}}_c \tag{7}$$

where $\overline{\rho}$ is the mean gas density, ν and ν_t are the molecular kinematic and turbulent viscosities, Sc_t (= 0.7) is the turbulent Schmidt number and $\overline{\dot{w}}_c$ is the mean reaction rate. The latter is modelled often with the assumption, to be a product of laminar reaction rate ($\rho_u S_{L0}$) and turbulent flame wrinkling

$$\overline{\dot{w}}_c = \rho_u S_{L0} I_0 \Sigma. \tag{8}$$

Here S_{L0} is the unstretched laminar burning velocity, I_0 is the flame stretch factor, accounting for curvature influences, and Σ the average flame surface density [15, 16].

In general, for any algebraic model the common formulation of density-averaging relating density of the gas and progress variable are based on the following assumptions. For a given expansion ratio, relations for the instantaneous and mean density may be readily obtained, using the relations:

$$\rho = \frac{\rho_u}{(1+\tau c)}\ ;\quad \overline{\rho} = \frac{\rho_u}{(1+\tau \tilde{c})}\ ;\quad \tau = \frac{T_u}{T_b} - 1 \tag{9}$$

where τ is the heat release parameter.

2.3 Models of Bray-Moss-Libby and Lindstedt-Váos

In the Bray Moss Libby (BML) model [17] the flame surface density is modeled using the following relation

$$\Sigma = \frac{g}{\sigma_y}\frac{\overline{c}(1-\overline{c})}{L_y};\quad L_y = C_l\, l_x \left(\frac{S_{L0}}{u'}\right)^n \qquad (10)$$

$$where,\ \ g = 2.0,\ \ C_l = 1.0,\ \ n = 1.0,\ \ \sigma_y = 0.5$$

The flame stretch factor (I_0) is calculated as follows

$$I_0 = \frac{0.117}{1+\tau} Ka^{-0.784} \quad with \quad Ka = 0.157\left(\frac{u'}{S_{L0}}\right)^2 \mathrm{Re}_t^{-1/2} \qquad (11)$$

Lindstedt and Váos [18] proposed an algebraic closure expression for the flame surface density, derived on the presumption that the flamelet geometry is fractal i.e. based on the length scale cut-off limits. The inner cut-off is taken to be equal to the Kolmogorov length scale (η) and outer cut-off equal to the turbulent integral length scale (l_x). The probability of reaction occurring at $\tilde{c}(x)$ is taken to be proportional to $\tilde{c}(1-\tilde{c})$. With the assumption that the fractal dimension D is equal to 7/3 and introducing the Kolmogorov velocity V_K, the Lindstedt and Váos (LV) model is closed with the mean reaction rate expression

$$\overline{w}_c = C_R \rho_u \frac{S_{L0}}{V_K}\frac{\tilde{\varepsilon}}{\tilde{k}}\tilde{c}(1-\tilde{c}) \qquad (12)$$

$$with\ \ C_R = 2.6,\ \ V_K = (\varepsilon\nu)^{1/4}$$

2.3. Turbulent Flame Speed Closure (TFC) and Algebraic Flame Surface Wrinkling (AFSW) models

Two other approaches are also based on Eq. (8). In the turbulent flame speed closure (Zimont and Lipatnikov) the laminar flame speed and the turbulent wrinkling factor are combined to a generalized turbulent flame speed (being now interpreted as a field variable) and a gradient-c-term, describing the location of the average reaction zone [19, 20]

$$\overline{w}_c = \rho_u S_T \left|\nabla\tilde{c}\right| \qquad (13)$$

which is used in original or extended version in various studies, e.g. in [21, 22].

The turbulent flame speed in the original Turbulent Flame Speed Closure (TFC) is modelled with a following algebraic relation, being derived from experimental data, theoretical argumentations and fitting [20] with assumed validity for highly turbulent flames

$$S_T = 0.52\, u'^{0.75} S_{L0}^{\ 1.5} \alpha^{-0.25} l_t^{0.25} \qquad (14)$$

In comprehensive adjustment work another relation is found from Muppala et al. [23], being validated also for lower turbulence situations and for a broad range of lean methane, ethylene or propane flames [24] at pressures up to 1.0 MPa. With the average reaction term being interpreted as a flame surface wrinkling factor, this so called Algebraic Flame Surface Wrinkling (AFSW) model [23]) is formulated as

$$\overline{w}_c = \rho_u S_{L0} \left(A_T / \overline{A}\right)\left|\nabla\tilde{c}\right| \qquad (15)$$

with the closure being

$$\frac{A_T}{\overline{A}} = \frac{S_T}{S_{L0}} = 1 + \frac{0.46}{\exp(Le\text{-}1)} Re_t^{0.25}\left(\frac{u'}{S_{L0}}\right)^{0.3}\left(\frac{p}{p_0}\right)^{0.2} \qquad (16)$$

Here a separate pressure dependency term p/p_o (with p_o = 1 bar) is included, fitting well to the broad set of data. It is notable, that here the Lewis number Le has been found to account for different pure gaseous fuels of lean mixtures [23]. Here, u' is the rms-velocity fluctuation (calculated from k) while the turbulent Reynolds number is $Re_t = u'\, l_x/\nu$ with the integral length scale l_x (calculated from k and ε) and the kinematic viscosity ν. In several numerical studies this model has been found to be reasonably predictive for different experimentally defined turbulent premixed flames [25, 26], even in LES models [27].

The finding of this explicit and first order dependency of the average reaction rate from the Lewis number (note that for $Le \approx 1$ the Taylor expansion leads to $\exp(Le\text{-}1) \approx Le$) was fully unexpected, as is mentioned in the introduction. More specifically effects on the local reaction rate in curved flames coming from unbalanced molecular transport between heat (towards the unburnt side) and fuel (from the unburnt side towards the reaction zone) are likely. However, they should cancel out for the positively and negatively curved flame elements inside a turbulent flame brush. From the relation (16), being derived from a large set of experiments, it was therefore concluded that the flame propagation is more dominated from the positively curved flame elements, being near the leading side of the turbulent flame brush [13], while the negatively curved flame elements are of minor importance. This picture has similarities to the leading point concept proposed from older Russian studies (Zeldovich [28], Kuznetsov and Sabel'nikov [29], see also the review from Lipatnikov and Chomiak [12]).

2.4. Modelling turbulent methane/hydrogen combustion with an effective Lewis number

For methane/hydrogen/air flames, a recent study shows that this rather simple AFSW model can be still used, if the Lewis number term in the equation 16 is modified to an effective Lewis number of the mixture,

$$\frac{A_T}{\bar{A}} = \frac{S_T}{S_{L0}} = 1 + \frac{0.46}{exp(Le_{eff} - 1)} Re_t^{0.25} \left(\frac{u'}{S_{L0}} \right)^{0.3} \left(\frac{p}{p_0} \right)^{0.2} \quad (17)$$

with the following relation for the effective Lewis number of the fuel mixture, being proposed by Dinkelacker et al. [13]

$$\frac{1}{Le_{eff}} = \frac{D}{\alpha} = \frac{x_{CH_4} D_{CH_4}}{\alpha} + \frac{x_{H_2} D_{H_2}}{\alpha} = \frac{x_{CH_4}}{Le_{CH_4}} + \frac{x_{H_2}}{Le_{H_2}} \quad (18)$$

where x_{CH_4} and x_{H_2} are the mole fractions of methane and hydrogen in the two-component fuel mixture. The assumption is a weighted diffusivity of the two fuel components $D_{eff} = x_{CH_4} D_{CH_4} + x_{H_2} D_{H_2}$, while the thermal diffusivity α remains nearly unaffected. The model behind this effective Lewis number approach is visualized in Figure 1.

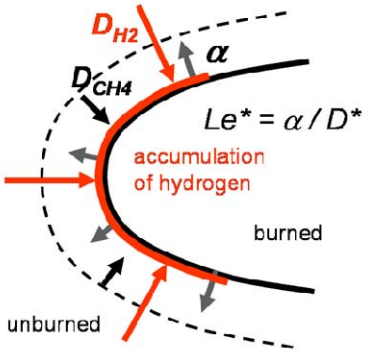

Fig. 1: Calculation of effective Lewis number based on a simplified description of the local molecular transport processes of the positively curved flame elements. The simple model of a weighted diffusivity of the fuel components leads to the effective Lewis number model described in the text.

Here the molecular transport processes near the positively curved "leading edge" flame elements are visualised. Due to the high diffusion coefficient of hydrogen the effective Lewis number varies significantly for the methane/hydrogen fuel mixtures investigated. Calculated Le_{eff} values of the mixture are given in Table 1 below.

Table 1. Experimental inflow conditions (U = 18 m/s, p = 0.1MPa) from Cheng et al. [5]

ϕ	H_2 vol %	ρ_u (kg/m^3)	ρ_b (kg/m^3)	T_{ad} (K)	Le_{eff}	S_{L0} (m/s)	α x 10^5 (m^2/s)	ν x 10^5 (m^2/s)
0.59	0	1.13	0.21	1610	0.960	0.104	2.00	1.61
0.4	40	1.11	0.24	1416	0.498	0.069	2.16	1.65
0.4	60	1.10	0.22	1495	0.402	0.116	2.30	1.66
0.4	80	1.06	0.21	1557	0.336	0.193	2.55	1.71
0.4	100	1.00	0.20	1614	0.290	0.302	3.05	1.81

It should be mentioned that other relations to determine an effective Lewis number for fuel mixtures (like proposed by Law et al. [30] for laminar flame studies) do not work for this turbulent combustion model.

To make the study more complete, we added such an effective Lewis number term also to the Lindstedt-Váos model. This follows earlier own work, as Aluri et al. [31] has found, that a tuned Lindstedt-Váos model with one added Lewis number term is rather predictive for methane and propane flames up to 10 bar, if the constant in Eq. 12 is modified to be

$$C_R = \frac{4.0}{e^{Le-1}} \quad (19)$$

Consequently we modified this term now also for the multi-component fuel/air mixtures with the effective Lewis number proposed in the frame of the AFSW model (Eq. 18).

$$C_R = \frac{4.0}{e^{Le_{eff}-1}} \quad (20)$$

In the following study, we use the name "tuned Lindstedt-Váos" (tLV) model here.

3 VALIDATION EXPERIMENTS

Recent experiments by Cheng et al. [5] on low-swirl burner (Fig. 2) investigated a range of lean CH_4/H_2/Air mixtures by varying hydrogen composition from 0 to 100 percent by volume, for varied pressures and velocities, operated partly even close to gas-turbine conditions. The test section has four 102 mm by 305 mm wide windows with a central combustor liner made of a 318 mm long quartz tube of 180 mm diameter. As shown in the schematic diagram, fuel and air are mixed before sending into the combustor and are also mixed with seeding particles for visualization. After mixing, the flow is passed through the flow homogenizer which has swirl and turbulence grid in another end of the pipe as shown in Fig. 2 and 3. The swirl section has 16 blades (with angle of 40°), and results in a swirl number of 0.5. The flow through the low-swirl injector (LSI) has two flow paths, the non-swirling middle portion with grid-induced turbulence and the outer swirling flow region. The outer swirling flow leads to flow divergence at the burner exit, allowing the flame to stabilize in the decreasing axial velocity field.

Table 1 shows the inflow conditions for the simulation test cases. The laminar burning velocity is calculated using the detailed GRI 3.0 reaction mechanism. The flow field data was obtained from PIV measurement. Data analysis was performed based on 224 image pairs for each flame condition. The experiments were carried out by generating natural gas flame at a given temperature, pressure, velocity and equivalence ratio. The hydrogen concentration is stepwise varied from 40%, to 60, 80 and 100%. Compared to other jet like configurations, this LSI flames are highly resistance to flash back and flame extinction. The current study is based on 0.1 MPa experiments with constant inflow velocity.

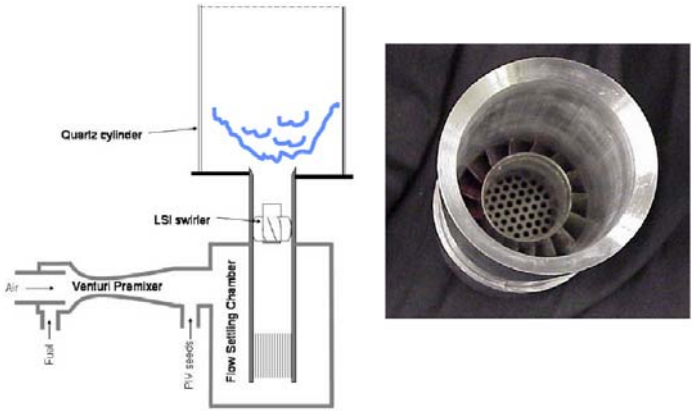

Fig. 2. Experimental schematic diagram and picture of the low swirl burner with turbulence grid and swirl blades, by Cheng et al. [5]

4 NUMERICAL GEOMETRY AND GRID DETAILS

For numerical simulation, the domain shown in Fig. 3 is considered, see also Fig. 4. The flow below the swirl grid is assumed to be completely homogeneous, and a 60 mm initial pre-chamber length is considered.

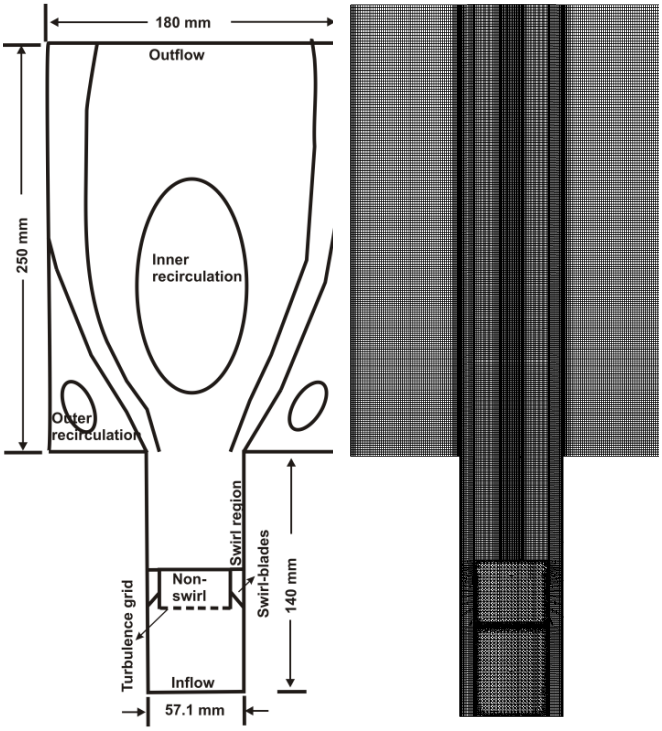

Fig. 3. Schematic diagram of the combustion chamber and the cross section of the numerical grid which is built out of tetrahedral cells in the middle and hexahedral cells in the swirl section and in the combustion chamber.

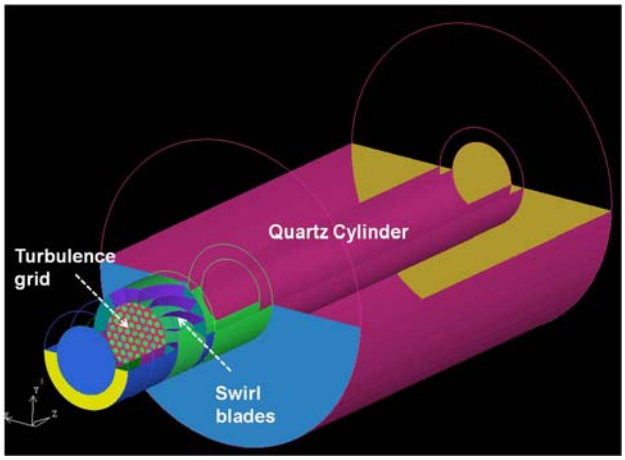

Fig. 4. Numerical geometry of the low swirl burner with 16 swirl blades, turbulence grid, and combustion chamber

The burner inlet diameter, combustion chamber diameter, chamber height are given in Fig. 3. Similar to the experimental configurations, the 16 swirl blades and approximately 52 turbulence holes are included into the simulation geometry to create the swirl and flow field similar to experiments. There are four divisions along the flow directions such as inlet section i.e. front part of swirl, turbulence blade and swirl section, connecting part between swirl and combustor, and combustion chamber. The radial direction is split into an inner core, the middle shear layer section, and an outer core in the combustion section. The grid is created with three O-grid steps in ICEM-CFD with 196 blocks. Cell sizes are 0.5 mm in the inner core, 0.3 mm in the shear layer and between 0.3 and 1.1 mm in the outer core section. Close to the combustor wall it reaches 0.5 mm, to get good wall y+ value. The total numbers of cells is 3.2 million. Numerical simulations are carried out with the ANSYS FLUENT CFD software. The reaction models are implemented as user-defined functions. Boundary conditions are determined according to the experiments. The RNG k-ε model with the default model constants is used for turbulence modelling. The considered boundary conditions are velocity inlet, outflow and wall. The operating conditions are tabulated in Table 1. The inflow conditions the turbulence intensity of 5% and a turbulent length scale of 1 mm are assumed in approximate accordance with experimental data.

5 RESULTS AND DISCUSSIONS

Calculation results are discussed in the following order: In the first part, the non-reacting flow inside the combustor is analyzed numerically, in order to understand the flow pattern of this combustor. Following that, the reaction closures are applied to pure methane flames, to see, if the reaction models work for situations where they are made for. The main part contains the numerical study of the methane/hydrogen combustion with hydrogen concentration between 40 and 100 by volume % of the fuel. Here the reaction models will be discussed stepwise, first those without, then those with inclusion of preferential diffusion effects.

5.1 Non-reacting flow comparison

In Figure 5 cold flow simulations are shown. The axial velocity reaches up to 26 m/s in the swirl region, the axial velocity is strongly localized at the outer side of the inlet section and reaches here about 21 m/s. At the exit of the inlet section, a vortex breakdown occurs which forms a rather large central recirculation region with an axial back flow velocity of up to –6 m/s. An outer recirculation zone re-attaches 60 mm above the inlet.

5.2 Reacting flow comparison

5.2.1 Pure methane flames

As a first step pure methane/air flames are calculated for the different reaction models. Figures 6 and 7 show the calculated flame positions and the axial velocity contours for all investigated reaction models. In each case the calculated flame is anchored approximately 30 mm above the combustor inlet. For this low swirl burner the flame stabilisation mechanism is based on the flow divergence coming from the swirling flow in the outer part. This results in a decrease of the axial velocity component on the burner axis. In Figure 8 the axial velocity is shown on the burner axis for both the experimental data as well as the predictions from the different reaction models. At about x = 40 mm the experimentally measured axial velocity shows a significant change of its decreasing trend before. It can be expected (not described in the experiments) that here the flame is anchored in the experiments (probably fluctuating and smearing the flame position and the measured average velocity to some extent), as the expansion in the flame front leads to a relative increase of the velocity in the burnt part. All numerical models predict the flame position also near to this position. It is expected that at this location the turbulent flame speed is equal to the axial convection speed leading to the stabilisation of the flame, approximately being around 2.5 to 3 m/s according to Fig. 8. It may be remarked that corresponding to the experimental observation this burner shows very stable operation for a broad range of conditions. Numerically simulations also predict a very stable flame for the set of cases studied, fitting to the observation that the details of the reaction rate model are of less importance for this flame.

The predicted pure methane flames by five reaction model show only small difference in flame and anchoring position in the middle axis as shown in the Fig. 6. Unlike the other reaction models, the BML model shows a different flame shape. Noticeably close to cylinder wall and in the outer recirculation zone it shows a partially burned mixture, while the other models predict fully burned gas. The experimental situation here is unfortunately not measured exact enough. However, it should be noted that in real experiments the outer wall is cooled, leading to decreased temperatures in the outer recirculation flow, which in any case is not modelled. Therefore we do not emphasise this difference between the BML model and the other models too much.

The flame shape predicted by AFSW reaction model is slightly longer in the region between inner and outer recirculation regions.

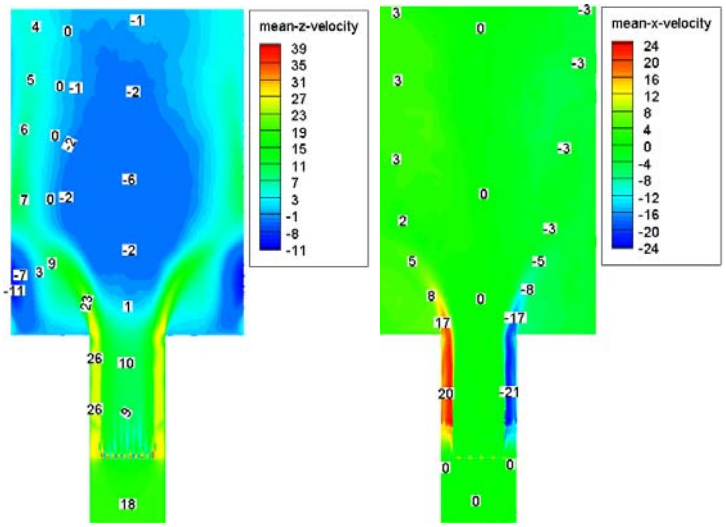

Fig. 5: Non reacting flow contours of axial (left) and radial (right) velocities for $U = 18$ m/s.

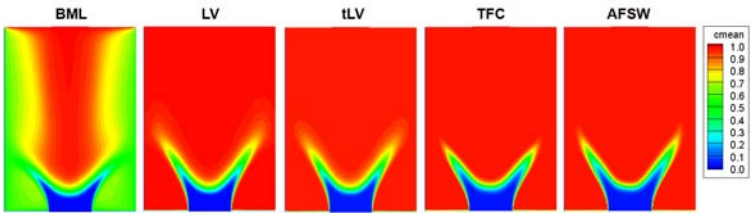

Fig. 6. Reacting flow: Mean reaction progress variable contours of pure methane flames with five reaction models at $\Phi = 0.59$, $U = 18$ m/s

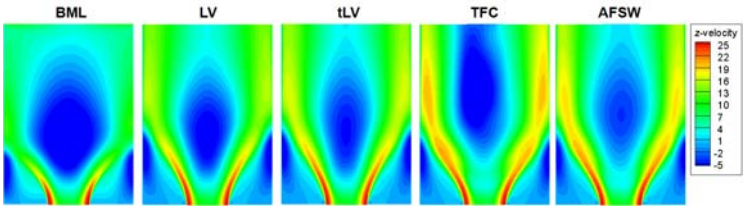

Fig. 7. Reacting flow: Mean axial velocity contours of pure methane flames with five reaction models at $\Phi = 0.59$, $U = 18$ m/s

Comparing the velocity contours for these pure methane flame, one can observe that the inner recirculation regions only slightly vary between the reaction models (Fig. 7). Among all the BML model shows a larger and broader region. The normalized axial velocity comparison (Fig. 8) shows that in the near field region of x < 40 mm, all the model predict the experimental behaviour, but in the later stages the predictions shows some deviations. Especially the BML and LV model results deviate largely with experimental predictions. The AFSW model prediction is in good agreement with experiment compared to the other models.

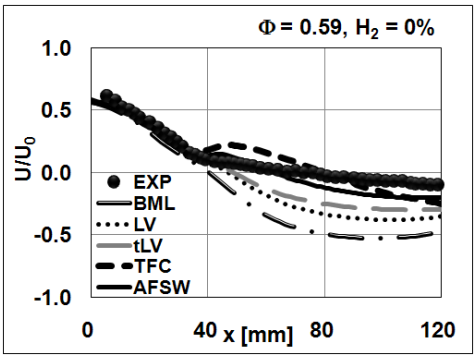

Fig. 8. Axial profile of the calculated axial velocity for pure methane, $\Phi = 0.59$. Five reaction models are compared with experimental data ($U_0 = 18$ m/s).

5.2.2 Hydrogen enriched methane flames predicted with the BML and LV models

In the following part of the study the amount of hydrogen is varied between 40 and 100 by volume percent. In the first section, the BML and LV models predictions are shown, as both are based on the $\overline{c}(1-\overline{c})$ relation in the reaction source. In the second part, those models being based on a gradient closure of the progress variable $|\nabla\tilde{c}|$ are compared, such as the TFC and the AFSW reaction model. So far all these models do not contain an explicit Lewis number effect (for comparison, in the AFSW model Le = 1 is assumed for all mixtures, to allow the separated analysis of the hydrogen influence on laminar flame speed being included without an influence of preferential diffusion). In the last section two models are compared where the explicit influence of preferential diffusion is included in an explicit Lewis number term, comparing the tuned LV model (tLV) and the AFSW reaction model.

In this first part of the reacting flow comparisons, the BML and the LV reaction model predictions are discussed for the varied hydrogen concentrations (40, 60, 80 and 100% of the fuel mixture). The equivalence ratio of 0.4 is hold constant, as well as inflow velocity and turbulence is constant. The BML model predictions show an increased reactivity with hydrogen addition, but the flame anchoring position or shape does not show any noticeable difference with hydrogen addition. However, with the BML model, another phenomenon is well observed. i.e. the high diffusivity of hydrogen promotes burning in the outer shear layer and this creates a high velocity region. This is similar to the experimental findings of Cheng et al. [5] in which increase of hydrogen leads to increased OH concentration in the outer recirculation region. The flame contour of 60 % H_2 starts to display the increase of reactivity in the outer recirculation region. For the LV reaction model, the flame shape in the region between central and outer

recirculation zone becomes smaller with increase of hydrogen concentration from 40 to 100 %. This increase of reactivity is due to increase of unstretched laminar burning velocity (S_{L0}) in the reaction rate equation.

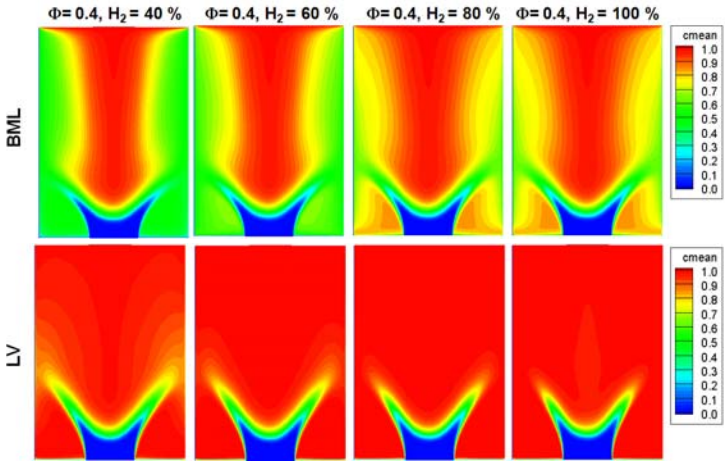

Fig. 9. Reacting flow: Mean reaction progress variable contours of 40, 60, 80 and 100% hydrogen enriched methane flames with BML (top) and LV (bottom) reaction models at Φ = 0.4, U = 18 m/s

The simulated velocity contours shown in Fig. 10 reveals that the predicted inner recirculation region using the BML model does not show any change with hydrogen concentration. The LV model shows a slight change of the size of the central recirculation zone due to increase in heat release with hydrogen addition.

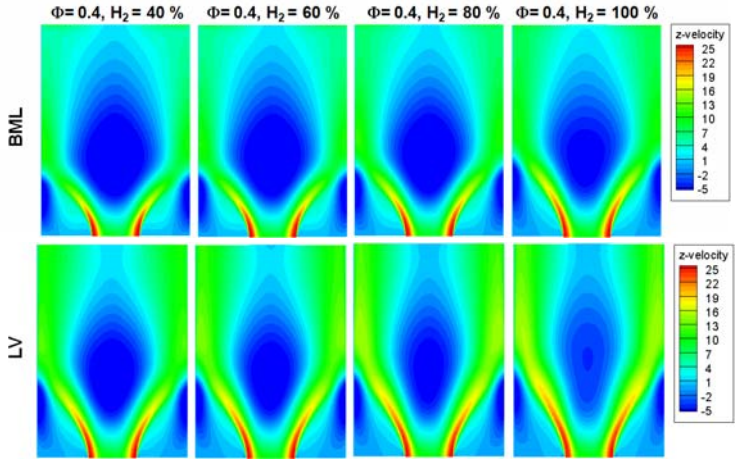

Fig. 10. Reacting flow: Mean axial flow velocity contours of 40, 60, 80 and 100% hydrogen enriched methane flames with BML (top) and LV (bottom) reaction models at Φ = 0.4, U = 18 m/s

The predicted axial flame anchoring position on the axis of the burner remains nearly unchanged for both models. Here a deviation to the experimental flame position can be seen in Figure 11 for higher hydrogen concentrations. Experimentally the flame anchoring position moves upstream for 80 and 100 % hydrogen and also the axial velocity profile shows now a significant increase of axial velocity in the burnt part. Both are not predicted with these two models.

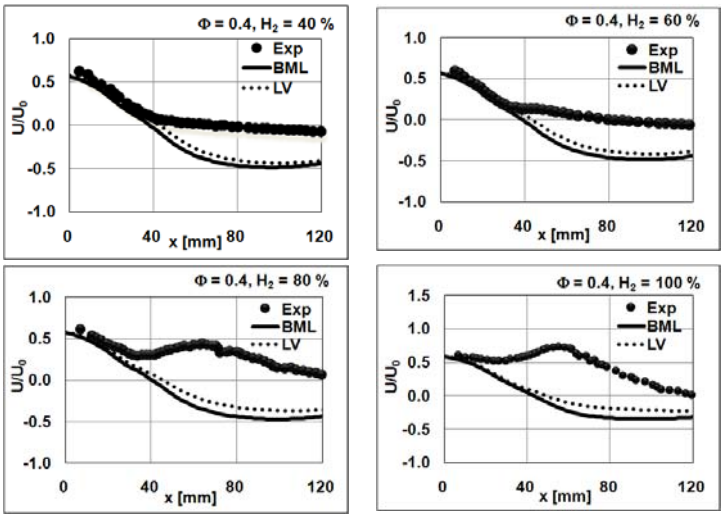

Fig. 11. Reacting flow: Normalized mean axial flow velocity comparison along the middle axis for 40, 60, 80 and 100% hydrogen enriched methane flames with BML (top) and LV (bottom) reaction models at Φ = 0.4, U = 18 m/s

5.2.3 Hydrogen enriched methane flames predicted with the TFC and the AFSW model without Lewis number

Both the TFC and the AFSW reaction model are based on an algebraic turbulent flame speed relation, which is locally determined as a function of the local turbulence quantities. In the comparison of this section, the AFSW model is artificially simplified, as the Lewis number value is assumed to be unity (Le = 1.0), so both models are similar in structure. With this unity Lewis number assumption, the simulations are carried out for all the four hydrogen concentrations.

The flame contours (Fig. 12) predicted by both TFC and AFSW reaction models show an increased reactivity with increase of hydrogen concentration, which leads to smaller flame size. Though both models show a similar trend, a small difference can be observed in the reaction progress variable flame contours. In this formulation, only the increase of the unstretched laminar burning velocity (S_{L0}) is included in the prediction of the overall reaction rate.

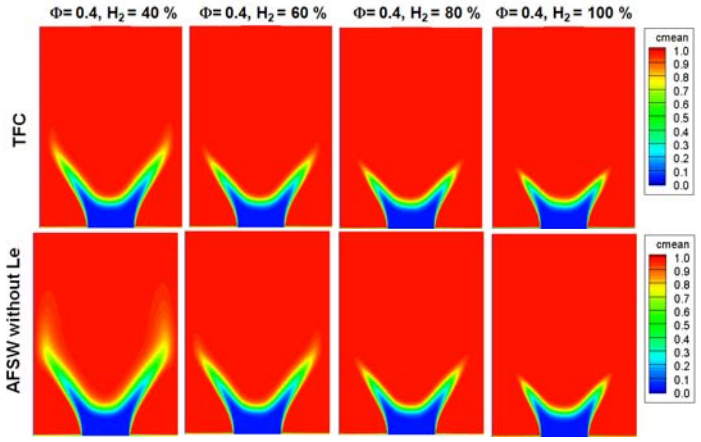

Fig. 12. Reacting flow: Mean reaction progress variable contours of 40, 60, 80 and 100% hydrogen enriched methane flames with TFC (top) and AFSW without Le (bottom) reaction models at Φ = 0.4, U = 18 m/s.

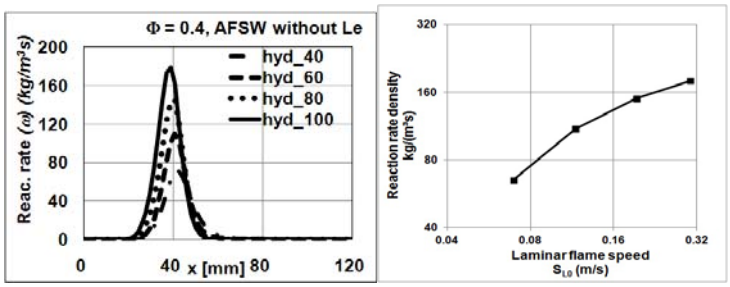

Fig. 13. Reacting flow: a) Mean reaction rate predictions of AFSW without *Le* model for 40, 60, 80 and 100 % hydrogen concentration at Φ = 0.4, U = 18 m/s (left). b) Log-log scaling of reaction rate as function of laminar flame speed (right).

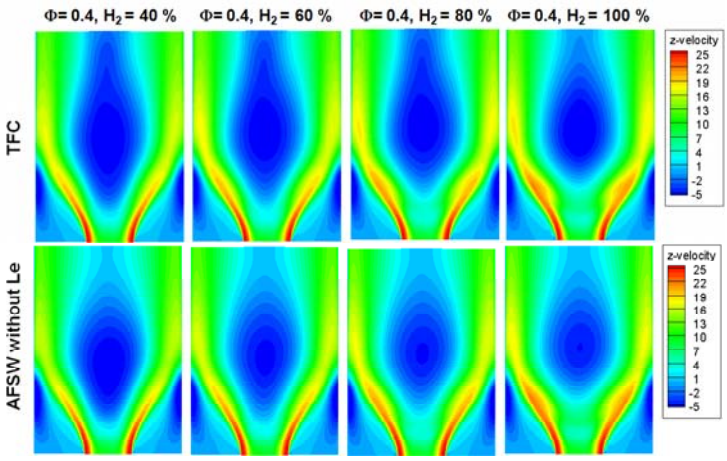

Fig. 14. Reacting flow: Mean axial flow velocity contours of 40, 60, 80 and 100% hydrogen enriched methane flames with TFC (top) and AFSW without Le (bottom) reaction models at Φ = 0.4, U = 18 m/s

Comparisons of the mean axial velocities contours in Figure 14 predict that the inner recirculation region shape changes to some extent with addition of H_2.

In Figure 15 the normalized axial velocity is compared with measured data on the middle axis. Both the TFC and the AFSW (without *Le*-effect) model show that the flame position moves upstream for increased hydrogen content, being in agreement with the experimental data, if the minimum of the axial velocity (visible for 80 and 100 % H_2) is taken as flame position. However, the predicted increase of velocity is much lower than the measured velocity.

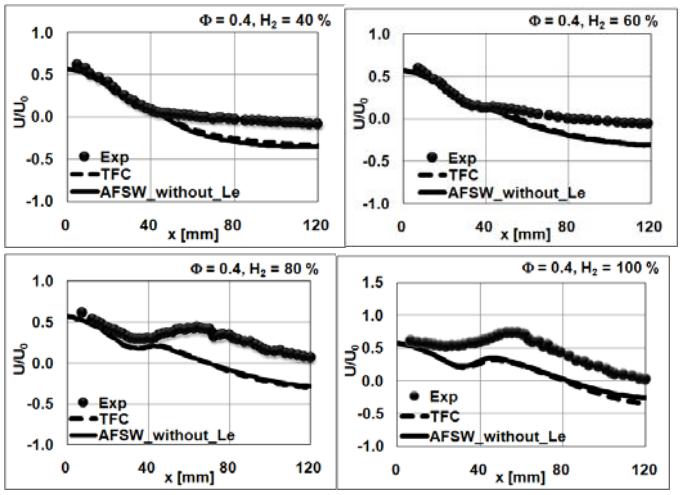

Fig. 15. Reacting flow: Normalized mean axial flow velocity comparison along the middle axis for 40, 60, 80 and 100% hydrogen enriched methane flames with TFC (top) and AFSW without Le (bottom) reaction models at Φ = 0.4, U = 18 m/s.

5.2.4 Hydrogen enriched methane flames predicted with the tLV and the AFSW model including an effective Lewis number term

As the third part of this study two models are investigated where an explicit dependency on the effective Lewis number is included. For the AFSW model this extension was proposed by Dinkelacker et al. [13], being tested with good success on high pressure Bunsen flames from Orléans with methane/hydrogen mixtures with hydrogen content up to 20 and partly up to 40 percent [13]. This relation is used here for predictions of the low swirl burner flames for higher hydrogen concentration. Additionally the tuned Lindstedt-Váos (tLV) model is used according to Eq. (20).

In Figure 16 the calculated flame positions are shown for the tLV and the AFSW model, wherein preferential diffusion effects are included with the effective Lewis number. With both models the flame position moves upstream with increased

hydrogen content. This shows that the reaction rate increases - according to the expectation. Also the flame size decreases, indicating the same trend.

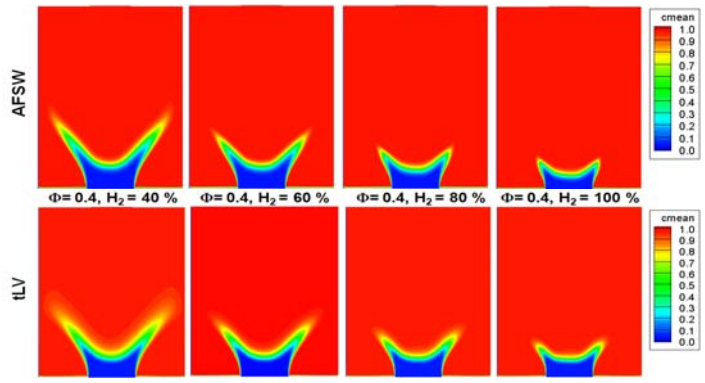

Fig. 16. Reacting flow: Mean reaction progress variable contours of 40, 60, 80 and 100% hydrogen enriched methane flames with tLV (top) and AFSW with effective Le (bottom) reaction models at Φ= 0.4, U = 18 m/s

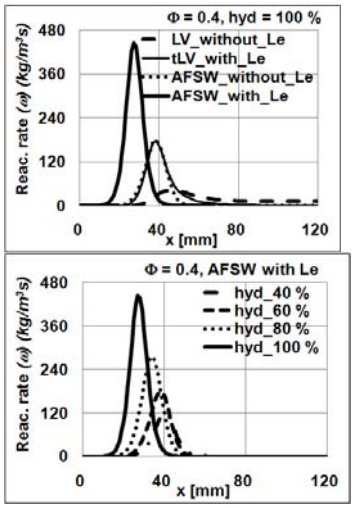

Fig. 17. Reacting flow: Mean reaction rate predictions of LV, tLV, AFSW models with and without Le term for 100 % hydrogen concentration (left) and similar comparison using AFSW with Le (right) for variation of hydrogen concentration at Φ = 0.4, U = 18 m/s

In Fig. 17 the reaction rate profiles along the axis are shown for different hydrogen concentrations (right side) for the AFSW model. With increased hydrogen concentration the movement of the flame position can be seen (compare with Fig. 13, where this movement was only small). Additionally the predicted reaction rate increases significantly with hydrogen concentration and reaches a maximum value of 460 kg/m3s. This is approximately three times higher than the rate predicted by the AFSW without the Lewis number term (see left side plot in Fig. 17). Here, the influence of the explicit Lewis number term is clearly visible. This trend holds also for the tLV model. The profiles show that here the reaction rate values are lower and the position of the reaction zone is located about 15 mm downstream.

The calculated velocity contours are shown in Fig. 18, and in Fig. 19 the predicted axial velocity profiles can be compared with the measured data.

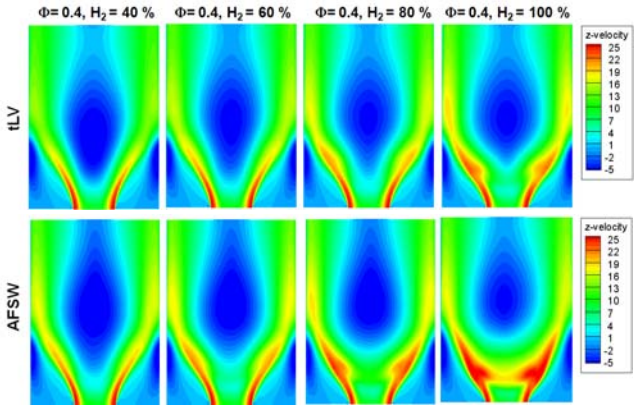

Fig. 18. Reacting flow: Mean axial flow velocity contours of 40, 60, 80 and 100% hydrogen enriched methane flames with TFC (top) and AFSW without Le (bottom) reaction models at Φ = 0.4, U = 18 m/s

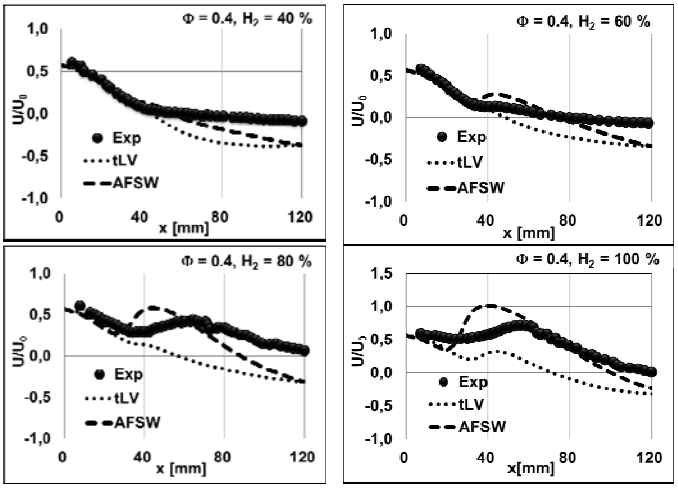

Fig. 19. Reacting flow: Normalized mean axial flow velocity comparison along the middle axis for 40, 60, 80 and 100% hydrogen enriched methane flames with tLV and AFSW with effective Le reaction models for Φ = 0.4, U = 18 m/s

For 80 and 100 percent hydrogen the AFSW model predicts now a significant increase of the axial velocity in the reaction zone, indicating the effects of this concentrated heat release and being generally in accordance with the experimental measurements. The positions are relatively similar to the experimental values, although the measured values are

more spread (maybe due to larger scale fluctuations of the flame front which is not much included in the RANS modelling approach). For pure hydrogen the tLV model shows an increase of the axial velocity. In the burnt part of the flames the AFSW model is, however rather well fitting to the experimental profile, which is less the case for the tLV model. In Figure 18 the increase of axial velocity is seen also in the two-dimensional presentation. In conjunction with the increased and more localized heat release zone the overall flow field and the region of recirculation is affected clearly. It would be allowed to carry out further validation studies should more experimentally data would have been available than just the axial velocity profiles.

Concluding this comparative study it was shown that all investigated reaction models can predict roughly the studied low swirl flames for varied hydrogen concentration. However, as this flame is inherently very stable due to the swirl induced inner recirculation zone, also the sensitivity is rather low to differences of the modelling terms. Looking to more details, especially the experimental axial velocity profiles along the burner axis are available differences between the models can be found for the investigated fuel mixtures. The models proposed for single fuels, like the BML and the LV model, and also the TFC model, show more deviations from the experiment. The first two models do not even show the increased flow velocity on the axial profile. Both the TFC and AFSW models without the extra Lewis number term, with exclusion of additional preferential diffusion effects in curved flame elements (similarly also in strained flame elements[11]) are already to some extent more predictive even for the fuel mixtures. However, inclusion of an extra Lewis number term using an effective Lewis number is better usable for a broad range of methane/hydrogen fuel mixtures. The modified version of the AFSW model shows also near accurate flow velocity in the burnt part behind the flame front. This is a strong indication that indeed preferential diffusion effects are of great importance also for highly turbulent flames.

6. CONCLUSION

Reaction modelling of turbulent methane/hydrogen combustion is important for several potential application fields. It is a possible flex-fuel mixture in combustion devices like gas turbines and gas engines, if regeneratively produced hydrogen is added to the existing natural gas system in varied amount to work as huge energy storage for strongly varying energy production rates from renewable energies like wind and solar energy. Another vision is the hydrogen future being an energy carrier with CO_2 free combustion emission. However the direct use of hydrogen may be limited due to its high diffusivity, reactivity and burning velocity, so methane/hydrogen blends may be reasonable solutions. In the current study, therefore the extension of premixed turbulent reaction rate models for hydrogen/methane fuels is investigated. For that, different numerical models are compared on a set of experiments done on the low swirl burner of Cheng et al. The results are compared with experimental data, where the mean flow velocity and inflow turbulence is hold constant, while the fuel/air mixture is varied with hydrogen concentrations of 40, 60, 80, and 100 percent hydrogen in methane of the lean flames.

Problematic is especially the modelling of the averaged reaction rate in turbulent premixed combustion. The basic assumption of such models is often that the averaged turbulent reaction rate is the product of a laminar reaction rate and a turbulent flame wrinkling factor. If modelling turbulent hydrogen or hydrogen/hydrocarbon combustion it may be assumed that the specific effects of higher reactivity for hydrogen are already included in the laminar reaction rate.

Three of the investigated models (from Bray-Moss-Libby, Lindstedt-Váos, and the turbulent flame speed closure model) and within this study also the artificially shortened AFSW model are based on this assumption. The comparison with the experimental data shows that this assumption does not hold. Even for constant turbulence conditions, the addition of hydrogen to the fuel leads to effects not being described alone with the modified laminar burning velocity.

As is discussed in the recent years with experiments, theory and detailed numerical studies, additional effects are of importance. Recently, we developed an extended version of the algebraic flame surface wrinkling model (AFSW model) where with an explicitly included Lewis number term effects of molecular diffusion are seen to be important even in highly turbulent flames. The knowledge of such effects for laminar flame instabilities is old. However, for highly turbulent flames this was against the expectation, that here turbulent transport would be much more significant than molecular transport. For the methane/hydrogen mixture a new relation for an effective Lewis number was proposed, being based on the weighted average of the fuel diffusivities (for lean mixtures). It is shown in this study that this model works much better than the other mentioned model, being nearly predictive for the investigated combustion situations. Also, one of the firstly mentioned model (LV model) was tuned in the way that this effective Lewis number term was included as a prefactor (tLV model). Being somewhat less accurate this tLV model is found to be rather predictive as well.

This numerical study clearly demonstrates the importance of preferential diffusion and Lewis number effects on the

predictions of hydrogen enriched hydrocarbon flames. The reached status of predictivity is already relatively high for lean fuel/air mixtures, so the chance is that combustion devices like gas turbines and/or gas engines for flame safety situations can be calculated based on this kind of modelling approach.

NOMENCLATURE

A	average burning area (m^2)
A_T	turbulent burning area (m^2)
c	reaction progress variable (0 unburned, 1 burned)
h	mole fraction of hydrogen in the fuel mixture
I_0	stretch factor
k	turbulent kinetic energy (m^2/s^2)
Ka	Karlovitz number
Le	Lewis number (α/D)
Le_{eff}	effective Lewis number of deficient component mixture
l_x	integral length scale (m)
L_y	length scale in Bray Moss Libby model
p	pressure (bar)
Re	Reynolds number
Re_t	turbulent Reynolds number (= $u'l_x\rho/\mu$)
Sc_t	turbulent Schmidt number (=0.7)
S_{ij}	strain rate magnitude (1/m)
S_{L0}	unstretched laminar burning velocity (m/s)
S_T	turbulent burning velocity (m/s)
T	temperature (K)
U	axial velocity (m/s)
u'	rms velocity fluctuation (m/s)
U_0	inflow velocity (m/s)
V	lateral velocity (m/s)
V_K	Kolmogorov velocity (m/s)

Greek

α	thermal diffusivity (m^2/s)
D	mass diffusivity (m^2/s)
ε	dissipation rate (m^2/s^3)
ρ	density (kg/m^3)
μ	dynamic viscosity (kg/m s)
Σ	flame surface density (1/m)
τ	heat release rate
ν	molecular kinematic viscosity (m^2/s)
ν_t	turbulent eddy viscosity (m^2/s)
$\overline{\dot{w}_c}$	reaction rate per unit mass and unit time (kg/m^3s)

Subscript and superscript

u	quantity in unburned gas
b	quantity in burned gas

ACKNOWLEDGMENTS

The first author Dr Muppala would like to thank EPSRC for the Grant EP/H010173/1.

REFERENCES

1. Sarli, V. and Benedetto, A. Laminar burning velocity of hydrogen-methane/air premxied flames. Intern. J. of Hydrogen Energy, 2007. 32: p. 637-646.
2. Fairweather, M., Ormsby, M.P., Sheppard, C.G.W. and Woolley, R. Turbulent burning rates of methane and methane-hydrogen mixtures. Combustion and Flame, 2009. 156(4): p. 780-790.
3. Halter, F., Caractérisation des effets de l'ajout d'hydrogène et de la haute pression dans les flammes turbulentes de prémélange méthane/air, in Energétique - Mécanique des fluides. Doctoral Thesis 2005, l'Universite d'Orleans (France).
4. Griebel, P., Boschek, E., and Jansohn P. Flame stability and NOx emission improvements due to H2 enrichment of turbulent, lean premixed, high-pressure, methane/air flames. The Future of Gas Turbine Technology, 3rd Int. Conference, 2006. Paper No. S4 T2/1.
5. Cheng, R., Littlejohn, D., Strakey P.A., Sidwell, T. Laboratory investigations of a low-swirl injector with H2 and CH4 at gas turbine conditions. Proceedings of the Combustion Institute, 2009. 32(2): p. 3001-3009.
6. Schefer, R.W., Wicksall, D.M., and Agrawal, A.K. Combustion of Hydrogen-Enriched Methane in a Lean Premixed Swirl-Stabilized Burner. Proceedings of the Combustion Institute, 2002. 29: p. 843.
7. Shy, S., Chen, Y.C., Yang, C.H. Liu, C.C., Huang, C.M. Effects of H2 or CO2 addition, equivalence ratio, and turbulent straining on turbulent burning velocities for lean premixed methane combustion. Combustion and Flame, 2008. 153: p. 510-524.
8. Bell, J., Cheng, R.K., Day, M.S., Shepherd, I.G. Numerical simulation of Lewis number effects on lean Premixed Turbulent flames. Proceedings of the Combustion Institute, 2007. 31(1): p. 1309-1317.
9. Chakraborty, N. and Cant, S. Influence of Lewis number on curvature effects in turbulent premixed flame propagation in the thin reaction zones regime. Physics of Fluids, 2005. 17: p. 105105-105125.
10. Hawkes, E. and Chen, J. Direct numerical simulation of hydrogen-enriched lean premixed methane-air flames. Combustion and Flame, 2004. 138(3): p. 242-258.
11. Chakraborty, N., Klein, M., and Swaminathan, N. Effects of Lewis number on reactive scalar gradient alignment with local strain rate in turbulent premixed flames. Proceedings of the Combustion Institute, 2009. 32: p. 1409–1417.

12. Lipatnikov, A.N. and Chomiak, J. Lewis Number Effects in Premixed Turbulent Combustion and Highly Perturbed Laminar Flames. Combusion Science and Technology, 1998. 137: p. 277-298.
13. Dinkelacker, F., Bhuvaneswaran, M. and Muppala, S.P.R. Modelling and simulation of lean premixed turbulent methane/hydrogen/air flames with an effective Lewis number approach. Combustion and Flame, 2011. 158(9): p. 1742–1749.
14. Fluent. Computational Fluid Dynamics Software, in ANSYS Fluent Incorporated, Lebanon, NH, USA. 2009.
15. Bray, K., Turbulent Flows with Premixed Reactants, in Turbulent Reacting Flows, P.A. Libby and F.A. Williams, Editors. 1980, Springer: Berlin. p. 115-183.
16. Poinsot, T. and Veynante, D. Theoretical and Numerical Combustion. 2001, Philadelphia: Edwards.
17. Bray, K.N.C., Libby, P.A. and Moss, J.B. Flamelet crossing frequencies and mean reaction rates in premixed turbulent combustion. Combust. Sci. Technol., 1984. 41: p. 143-172.
18. Lindstedt, P. and Váos, E.M. Modelling of premixed turbulent flames with second moment methods. Combustion and Flame, 1999. 116: p. 461-485.
19. Zimont, V.L., Theory of Turbulent Combustion of a Homogeneous Fuel Mixture at High Reynolds Numbers. Combust. Expl. and Shock Waves, 1979. 15(3): p. 305-311.
20. Zimont, V.L. and Lipatnikov, A.N. A numerical model of premixed turbulent combustion of gases. Chem. Phys. Reports, 1995. 14(7): p. 993-1025.
21. Dinkelacker, F. and Hölzler, S. Investigation of Turbulent Flame Speed Closure Approaches for Premixed Flame Calculation. Combustion Science and Technology, 2000. 158: p. 321-340.
22. Polifke, W., Flohr, P. and Brandt, M. Modeling of inhomogeneously premixed combustion with an extended TFC model. ASME, 2000. Paper No. 2000-GT-0135.
23. Muppala, S.P.R., Aluri, N.K., Dinkelacker, F., Leipertz, A. Development of an algebraic reaction rate closure for the numerical calculation of turbulent premixed methane, ethylene and propane/air flames for pressures up to 1.0 MPa. Combustion and Flame, 2005. 140: p. 257-266.
24. Kobayashi, H., Y. Kawabata, and K. Maruta, Experimental Study on General Correlation of Turbulent Burning Velocity at High Pressure. Proceedings of the Combustion Institute, 1998. 27: p. 941-948.
25. Aluri, N., Modelling of Molecular Effects and Dynamics of Turbulent Premixed Flames at Gasturbine Operating Conditions, in Department of Mechanical Engineering. Doctoral Thesis 2007, University of Siegen (Germany).
26. Muppala, S.P.R., Nakahara, M., Aluri, N.K., Kido, H., Wen, J.X. and Papalexandris, M.V. Experimental and analytical investigation of the turbulent burning velocity of two-component fuel mixtures of ydrogen, methane and propane. International Journal of Hydrogen Energy, 2009. 34: p. 9258-9265.
27. Aluri, N.K., Muppala, S.P.R. and Dinkelacker, F. Large-Eddy Simulation of Lean Premixed Turbulent Flames of Three Different Combustion Configurations using a Novel Reaction Closure. Flow Turbulence and Combustion, 2008. 80: p. 207.
28. Zel'dovich, Y.B., Barenblatt, G.I., Librovich, V.B., and Makhviladze, G.M. The Mathematical Theory of Combustion and Explosions. New York: Plenum, 1985.
29. Kuznetsov, V.R. and Sabel'nikov, V.A. Turbulence and Combustion. New York: Hemisphere, 1990.
30. Law, C.K., Jomaas, G. and Bechtold, J.K. Cellular instabilities of expanding hydrogen/propane spherical flames at elevated pressure: theory and experiment. Proceedings of the Combustion Institute, 2005. 30: p. 159-167.
31. Aluri, N., Muppala, S.P.R., and Dinkelacker, F. Substantiating a Fractal-based Algebraic Reaction Closure of Premixed Turbulent Combustion for High-Pressure and the Lewis Number Effects. Combustion and Flame, 2006. 145: p. 663-674.